

DOE/BC/14650--10

DE93 010065

73

A NOVEL APPROACH TO MODELING UNSTABLE EOR DISPLACEMENTS

Quarterly Report for the Period
October 1992—December 1992

NIPER Library
P. O. Box 2128
Bartlesville, OK 74005

Contract No. DE-AC22-90BC14650
The University of Texas at Austin
Austin, Texas

Contract Date: August 28, 1990
Anticipated Completion: August 27, 1993
Government Award: \$407,118 (Current Year)

Principal Investigator:
Ekwere J. Peters

Contracting Officer Representative:
Jerry D. Ham
Metairie Site Office
900 Commerce Road, East
New Orleans, Louisiana 70123

Prepared by
The University of Texas
Department of Petroleum Engineering
Austin, TX 78712

DISCLAIMER

This report was prepared as an account of work sponsored by an agency of the United States Government. Neither the United States Government nor any agency thereof, nor any of their employees, makes any warranty, express or implied, or assumes any legal liability or responsibility for the accuracy, completeness, or usefulness of any information, apparatus, product, or process disclosed, or represents that its use would not infringe privately owned rights. Reference herein to any specific commercial product, process, or service by trade name, trademark, manufacturer, or otherwise does not necessarily constitute or imply its endorsement, recommendation, or favoring by the United States Government or any agency thereof. The views and opinions of authors expressed herein do not necessarily state or reflect those of the United States Government or any agency thereof.

MASTER

DISTRIBUTION OF THIS DOCUMENT IS UNLIMITED

OBJECTIVES

This research is aimed at developing a methodology for predicting the performance of unstable displacements in heterogeneous reservoirs. A performance prediction approach that combines numerical modeling with laboratory imaging experiments is being developed.

Flow visualization experiments are being performed on laboratory corefloods using X-ray Computed Tomography (CT) and other imaging technologies to map the insitu fluid saturations in time and space. A systematic procedure is being developed to replicate the experimental image data with high-resolution numerical models of the displacements. The well-tuned models will then be used to scale the results of the laboratory coreflood experiments to heterogeneous reservoirs in order to predict the performance of unstable displacements in such reservoirs.

SUMMARY OF TECHNICAL PROGRESS

A new procedure has been developed to simplify the analysis, numerical modeling and scaling of laboratory coreflood experiments. The procedure consists of the following steps:

1. Image the coreflood by CT to obtain the temporal and spatial saturation profiles.
2. Transform the saturation profiles by means of a dimensionless self-similarity variable to obtain a unique, dimensionless response function that is characteristic of the coreflood.
3. History-match the characteristic response function for the coreflood with a numerical simulator.
4. After a satisfactory match, compare the experimental and computed saturation profiles and recovery curves for the coreflood.
5. Using the well-tuned numerical model, scale the results of the laboratory coreflood experiment to other systems.

Steps 1 through 4 of the above procedure were demonstrated in previous Quarterly Reports (Peters 1992a, Peters 1992b). In the first report, we derived a dimensionless self-similarity variable (x_D/t_D) for two-phase immiscible displacement and used it to transform the saturation profiles of two laboratory waterfloods in sandpacks to obtain their characteristic dimensionless response functions (steps 1 and 2). In the second report, we demonstrated steps 3 and 4 of the procedure by numerically simulating the two laboratory waterfloods. In a third report (Peters 1992c), we presented and discussed heterogeneous permeable media to be used in implementing step 5 of the procedure. In this report, we will present step 5 by scaling one of the laboratory waterfloods in a homogeneous sandpack to predict its expected performance in heterogeneous permeable media.

SIMULATION OF DISPLACEMENTS

In a previous report (Peters, 1992b), we successfully simulated an unstable waterflood experiment in a water-wet sandpack and calculated its dimensionless response curve (\hat{f}). A 2-D, x-z vertical cross-sectional grid of 53x122 was used to simulate the 3-D waterflood experiment. This grid was selected to coincide with the resolution of the 2-D slices of the CT images of the waterflood. The following similarity scaling groups were maintained the same in the simulation as in the experiment: viscosity ratio (μ_o/μ_w), capillary

number (N_c), gravity number (N_g), and stability number (N_s). The adjustable parameters used to accomplish the history-match were (1) the degree and structure of heterogeneity of the porous medium as measured by the Dykstra-Parsons coefficient and dimensionless correlation length, (2) the relative permeability curves (k_{rw} and k_{ro}), and (3) the capillary pressure curve (P_c). A Dykstra-Parsons coefficient of 0.05 and a correlation length of zero were used to characterize the laboratory sandpack. The relative permeability curves used in the simulation were based on the following analytical models.

$$k_{rw} = k_{wr} \left[\frac{S_w - S_{wi}}{1 - S_{wi} - S_{or}} \right]^{n_w} \quad (1)$$

$$k_{ro} = k_{or} \left[\frac{S_o - S_{or}}{1 - S_{wi} - S_{or}} \right]^{n_o} \quad (2)$$

The relative permeability parameters that gave the best match of the waterflood were $k_{wr} = 0.90$, $n_w = 3.5$, $k_{or} = 0.90$ and $n_o = 0.49$. The capillary pressure curve used in the simulation was

$$P_c = 0.01 \left[1 - \frac{S_w - S_{wi}}{1 - S_{wi} - S_{or}} \right]^2 \quad (3)$$

The numerical simulation was repeated in each of twelve heterogeneous media using the above relative permeability and capillary pressure curves. Table 1 lists additional parameters of the numerical simulations.

RESULTS AND DISCUSSION

Figure 1 shows the permeability maps for the twelve heterogeneous media used in the simulations. The degree and structure of the heterogeneity are characterized by the Dykstra-Parsons coefficient (DP) and the dimensionless correlation length (L_x). The Dykstra-Parsons coefficient ranged from 0.01 for a homogeneous medium to 0.87 for a highly heterogeneous medium. The dimensionless correlation length ranged from zero for a random permeability distribution to 2 for a highly correlated permeability distribution. It may be seen in Figure 1 that an increase in the correlation length of the permeability field results in an increasingly layered structure. Further, high L_x and DP give rise to heterogeneous media with structures similar to the sedimentary rocks of petroleum reservoirs. Thus, high L_x and DP permeability distributions typify petroleum reservoirs whereas low DP and high L_x distributions typify laboratory sandpacks.

Figure 2 compares the simulated dimensionless response function for each of the twelve heterogeneous media with that of the laboratory waterflood experiment. The following observations can be made from these results. If the heterogeneous media are characterized by low variability in the permeability distributions (low DP), the waterflood response will be essentially the same as in the laboratory sandpack regardless of the structure of the heterogeneity. This is indicated by the agreement between the simulated and the experimental response functions in the first column of Figure 2 (DP = 0.01). If the heterogeneous media are characterized by low correlation in the permeability distributions (low L_x), the waterflood response will be essentially the same as in the laboratory sandpack regardless of the variability in the permeability distributions. This is indicated by the agreement between the simulated and the experimental response functions in the first row of Figure 2 ($L_x = 0$). If the heterogeneous media are characterized by high variability and high

correlation in the permeability distributions, the waterflood response could be significantly different from that of the laboratory sandpack. This is most clearly shown by the response in the last permeability field in Figure 2 ($Lx = 2$ and $DP = 0.87$). In this case, the waterflood response is significantly less in the heterogeneous medium than in the laboratory sandpack. These observations are confirmed by the oil recovery curves shown in Figure 3.

We have investigated the reason for the significant disparity in performance between the laboratory waterflood in a relatively homogeneous sandpack and in certain kinds of heterogeneous media. The reason for this disparity can be seen in Figures 4 and 5 which show the simulated water saturation maps for each of the twelve heterogeneous media at 0.10 and 0.25 pore volumes injected. It is seen that the displacement in the heterogeneous media with high DP and high Lx are dominated by channeling of the injected water due to the permeability stratification. This results in significant bypassing of the oil in unswept layers and consequent low oil recovery. By contrast, the displacement in the media with low DP are characterized by excellent sweep comparable with that observed in the CT images of the laboratory waterflood experiment. This results in a displacement performance that is comparable to the laboratory waterflood experiment in the sandpack.

CONCLUDING REMARKS

In this report, we have presented the last step of a five-step procedure for modeling unstable displacements in heterogeneous permeable media. An unstable laboratory waterflood experiment in a homogeneous sandpack was scaled to predict its expected performance in heterogeneous media. It was found that the performance of the displacement in heterogeneous media could be significantly lower than in the laboratory experiment depending on the degree and structure of the heterogeneity of the media. This observation points to the need for proper scaling when using the results of laboratory coreflood experiments in relatively homogeneous media to forecast the expected performance in heterogeneous media. The five-step procedure we have developed and presented in this research can be used to accomplish this scaling and prevent erroneous performance forecasts.

NOMENCLATURE

DP	=	Dykstra-Parsons coefficient
\bar{f}	=	Dimensionless Response function
k_{rw}	=	Relative permeability to water
k_{ro}	=	Relative permeability to oil
k_{wr}	=	End-point relative permeability to water
k_{or}	=	End-point relative permeability to oil
Lx	=	Dimensionless correlation length in the x-direction
n_o	=	Relative permeability exponent for oil
n_w	=	Relative permeability exponent for water
N_c	=	Capillary number
N_g	=	Gravity number
N_s	=	Stability number
P_c	=	Capillary Pressure
S	=	Normalized water saturation
S_o	=	oil saturation
S_{or}	=	Residual oil saturation
S_w	=	Water saturation

S_{wi} = Connate water saturation
 t_D = Dimensionless time
 x_D = Dimensionless distance in the x-direction
 μ_o = Oil viscosity
 μ_w = Water viscosity

REFERENCES

- Peters, E.J.: "A Novel Approach to Modeling Unstable EOR Displacements," DOE Quarterly Report, January—March, 1992.
- Peters, E.J.: "A Novel Approach to Modeling Unstable EOR Displacements," DOE Quarterly Report, April—June, 1992.
- Peters, E.J.: "A Novel Approach to Modeling Unstable EOR Displacements," DOE Quarterly Report, July—September, 1992.

TABLE 1
SIMULATION CONDITIONS

	Simulation Data
Porous Medium	
Length	54.53 cm
Diameter	4.8 cm
Absolute Perm	9.26 darcies
Average Porosity	29.6 %
S_{wi}	0.15
Fluids	
Density of Displacing fluid	1.0882 g/cc
Viscosity of Displacing fluid	1.1276 cp
Density of Displaced fluid	0.9655 g/cc
Viscosity of Displaced fluid	103.4 cp
μ_o/μ_w	91.7
N_c	4.62×10^{-4}
N_g	1.26×10^{-3}
N_s	0.271×10^3

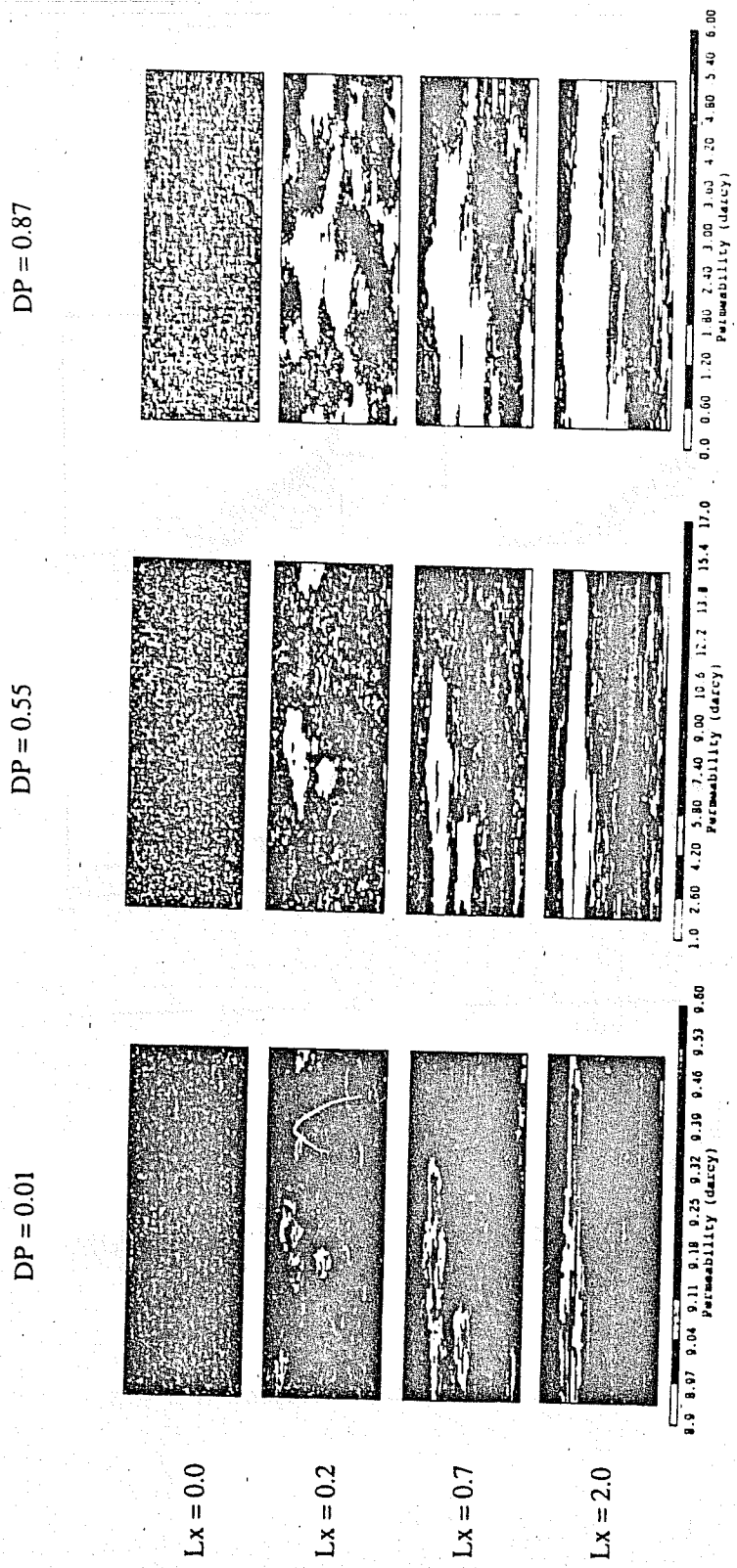


Figure 1 - Permeability maps

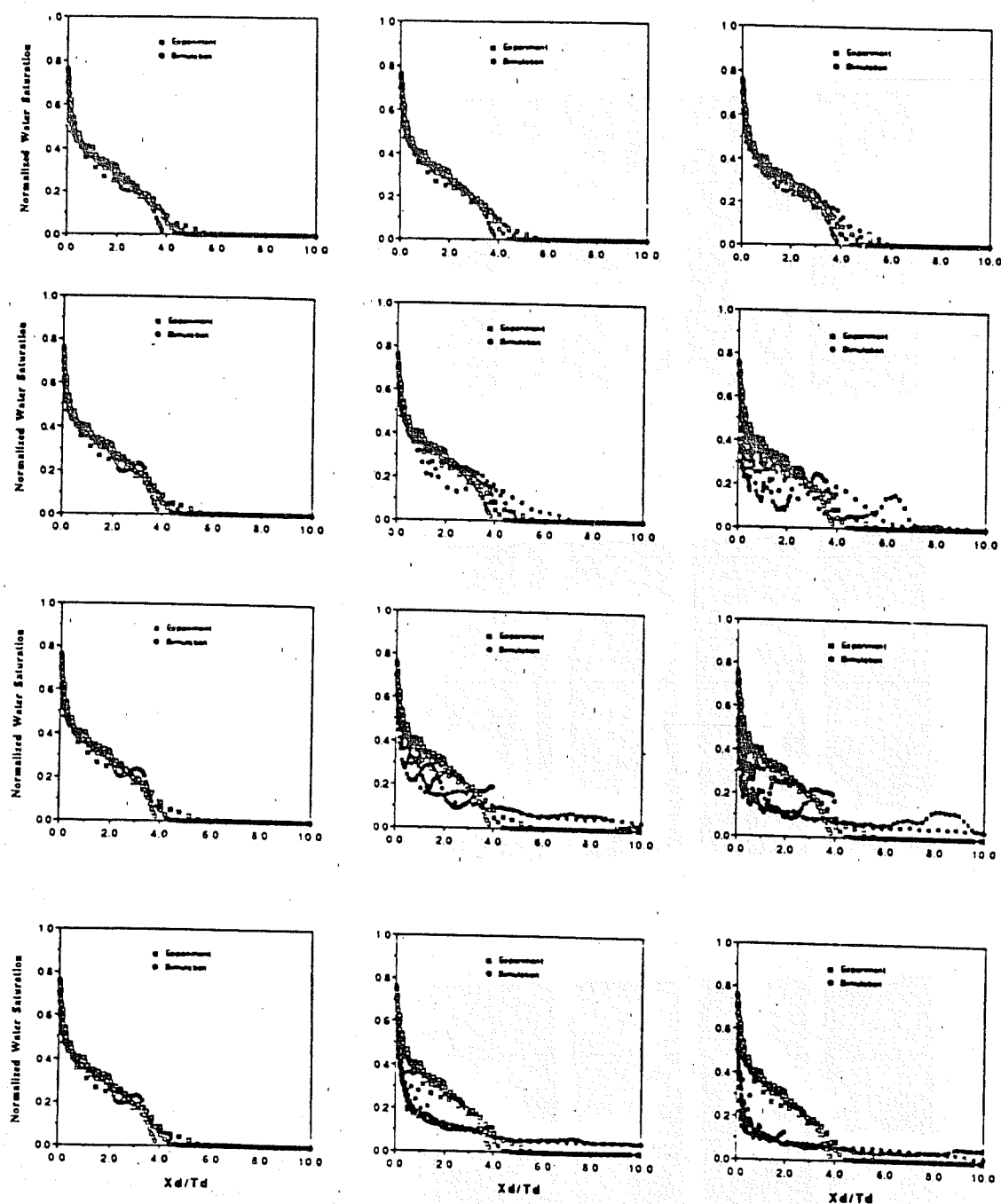


Figure 2 - A comparison of the experimental and simulated response functions

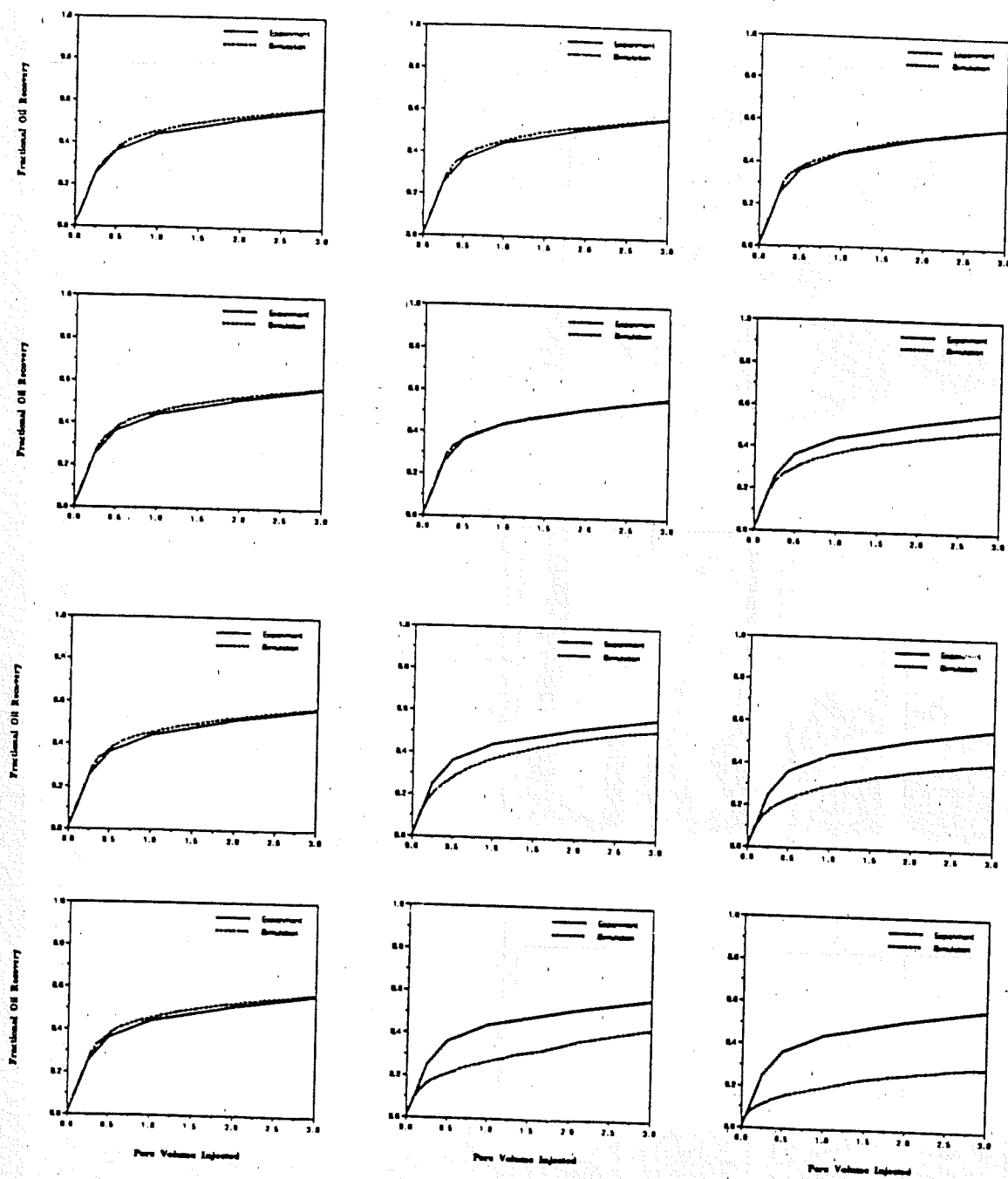


Figure 3 - A comparison of the experimental and simulated oil recovery curves

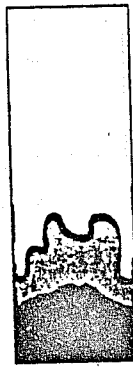
DP = 0.01



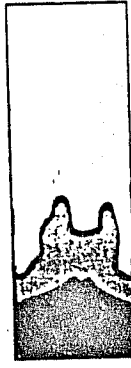
Lx = 0.0



Lx = 0.2



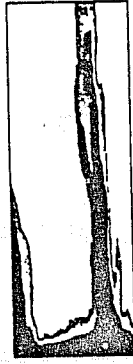
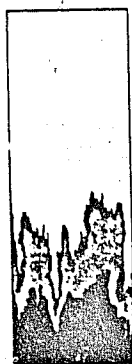
Lx = 0.7



Lx = 2.0

0.0 0.1 0.2 0.3 0.4 0.5 0.6 0.7 0.8 0.9 1.0
Water Saturation

DP = 0.55



0.0 0.1 0.2 0.3 0.4 0.5 0.6 0.7 0.8 0.9 1.0
Water Saturation

DP = 0.87



0.0 0.1 0.2 0.3 0.4 0.5 0.6 0.7 0.8 0.9 1.0
Water Saturation

Figure 4 - Simulated water saturation maps at 0.10 pore volume injected

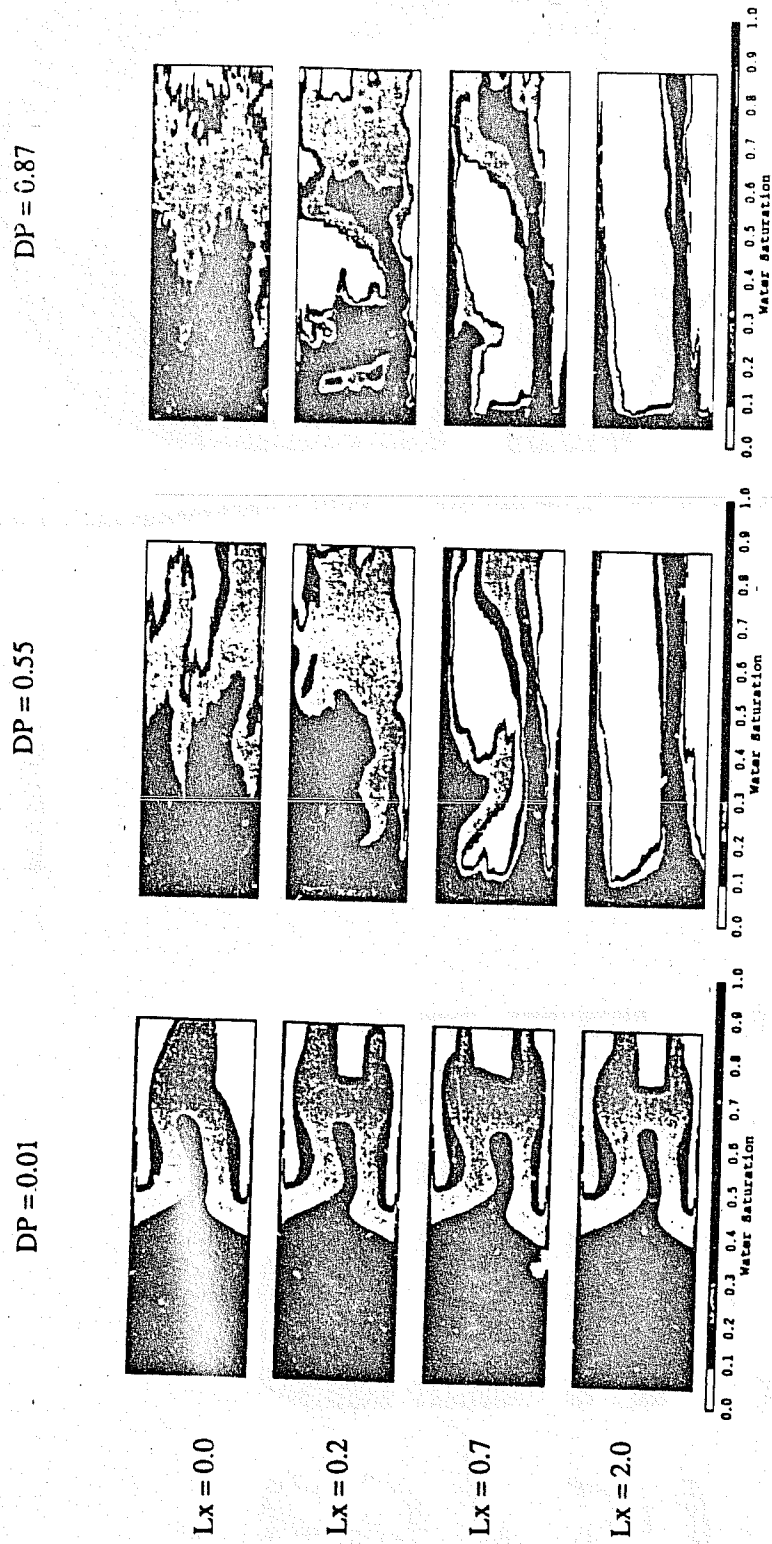


Figure 5 - Simulated water saturation maps at 0.25 pore volume injected

END

DATE
FILMED

4 / 15 / 93